Materials Science & Engineering A 706 (2017) 295–303

Contents lists available at ScienceDirect

Materials Science & Engineering A

journal homepage: www.elsevier.com/locate/msea

Role of alloying elements on twin growth and twin transmission in magnesium alloys

M. Arul Kumar[a,*], I.J. Beyerlein[b], R.A. Lebensohn[a], C.N. Tomé[a]

[a] Materials Science and Technology Division, Los Alamos National Laboratory, Los Alamos, NM 87545, USA
[b] Mechanical Engineering and Materials Department, University of California, Santa Barbara, CA 93106, USA

ARTICLE INFO

Keywords:
Alloy effect
Twin growth
Twin transmission
Microstructure

ABSTRACT

A spatially-resolved crystal plasticity Fast Fourier Transform (FFT)-based model is employed to study the effect of alloying addition on twin thickening and twin transmission in hexagonal close packed (HCP) magnesium. In the simulations, the influence of alloying additions is represented through the differences in the critical resolved shear stress (CRSS) of different slip and twinning modes. The results show that for the same grain orientation, twin type and boundary conditions, anisotropy in the CRSS values have a significant effect on twin thickening and twin transmission. Those with large differences in CRSS favor both twin thickening and twin transmission, and vice versa for those with small differences. However, less difference among the CRSS values enhances the dependence of thickening and transmission on the neighboring grain orientation.

1. Introduction

The plastic deformation of low-symmetry hexagonal close packed (HCP) metals and their alloys is accommodated through a combination of dislocation glide (slip) and deformation twinning [1–5]. The most commonly observed slip mode in HCP magnesium and its alloys is basal $\langle a \rangle$, with prismatic $\langle a \rangle$ and pyramidal $\langle c + a \rangle$ providing smaller shear contributions [1,3]. These slip modes operate in crystallographic planes and along crystallographic directions with different atomic density. As a consequence their activation barriers or critical resolved shear stress (CRSS) are not the same. The sensitivity of the plastic response of a crystal to its orientation increases with larger differences between the CRSS values for these slip modes. For a given Mg alloy, the ratios of CRSS values can change with strain and extrinsic variables like strain, strain rate and temperature [6] as well as microstructural variables, like grain size, lattice crystallographic orientation, stored dislocation structure, and impurities, etc [7–11]. However, comparatively these ratios can vary even more strongly among the different alloys of Mg. For instance, addition of Al and Zn in pure Mg [12], and the addition of Nd in Mg-1Mn [13] increases the CRSS for basal slip, which decreases the non-basal to basal CRSS ratio, and reduces its plastic anisotropy. Alloying of Mg with Li is believed to reduce the CRSS for $\langle c + a \rangle$ pyramidal slip [9,14]. These are just some of the numerous examples of how alloying can impact microscopically the CRSS ratios for slip and macroscopically the plastic anisotropy of the alloy [15,16].

Because twinning often operates in addition to slip, the effects of alloying on twinning are even less clear. To make the comparison it helps to consider the CRSS for twinning. The most common twin mode is the $\{10\bar{1}2\}$, while migration of the coherent twin boundary involves the motion of defects on the twin boundary [17,18], it is accepted that such migration is driven by a resolved shear stress (TRSS) on the twin plane and direction. Nucleation of a twin, on the other hand, is a local process driven by local stress states and dislocation reactions at grain boundaries [19]. We are not concerned with the latter process in this work. An effective (averaged) CRSS has been characterized along with the CRSS values of the slip modes operating alongside twinning. In doing so, the activation "strengths" for slip and twinning can be directly compared and propensity for twinning relative to slip estimated. Twinning can become favorable when its CRSS lies in between those for the distinct modes of slip or close to that of the easiest slip mode. For instance, WE43 and WE54 are rare earth Mg alloys exhibiting low plastic anisotropy, thought to be associated with an increase in the CRSS for twinning and a decrease in the CRSS for the non-basal slip modes [10,20]. Fig. 1 presents deformed microstructures of the AZ31 Mg alloy, pure Mg and the WE54 alloy, containing $\{10\bar{1}2\}$ tensile twins. For similar grain sizes and loading conditions, they developed significantly different amounts of twins, with ~ 50% twin area fraction in AZ31 Mg alloy at 3.9% strain, ~ 42% in pure Mg at 3.0% strain and < 5% in WE54 Mg alloy at 5% strain.

Apart from the average twinned area, details like whether twins are few and thick or numerous and fine or connected across neighboring grains can impact hardening. The harder pyramidal $\langle c + a \rangle$ slip system

* Corresponding author.
E-mail address: marulkr@gmail.com (M. Arul Kumar).

http://dx.doi.org/10.1016/j.msea.2017.08.084
Received 8 June 2017; Received in revised form 22 August 2017; Accepted 23 August 2017
Available online 24 August 2017
0921-5093/ Published by Elsevier B.V.

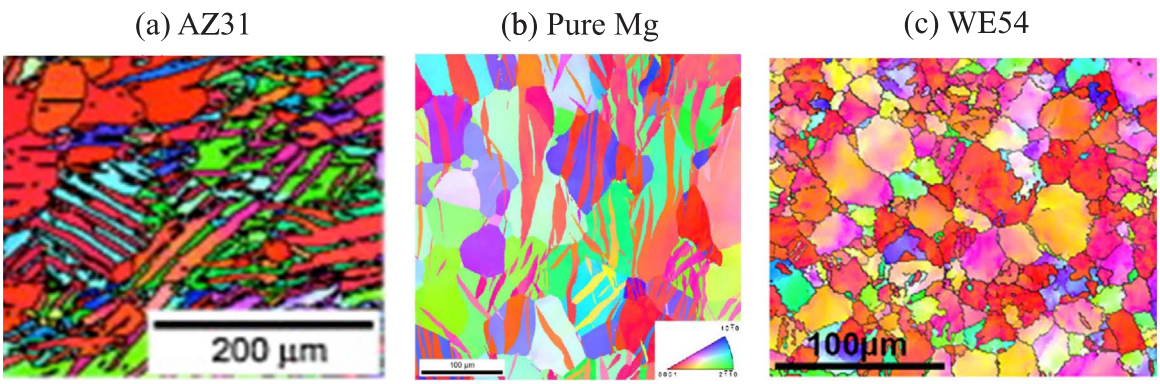

Fig. 1. Electron Back Scattered (EBSD) microstructural images of (a) AZ31 Mg alloy at 3.9% compressive strain (reprint from [21] with permission), (b) pure Mg at 3% compressive strain (reprint from [22] with permission), (c) WE54 Mg alloy at 5% compressive strain (reprint from [10] with permission). Despite the variation in initial texture, in all three cases, the imposed compression in a specific direction is the best way of loading the material to activate $\{10\bar{1}2\}$ tensile twins. The propensity for tensile twinning is high in AZ31 Mg alloy and in Pure Mg, and almost negligible in WE54 Mg alloy.

tends to be activated within thick twin domains [23–25]. Several thin twins can induce a separate hardening effect by introducing numerous twin boundaries that can hinder the glide of dislocations [26]. Twins that are connected across grain boundaries, or adjoining twin pairs (ATPs), can lead to the formation of fatigue cracks and premature failure [27–29].

It can be expected that alloying would affect the morphology of a twin while expanding within a grain. Twin propagation is driven by the stress state acting at its boundaries, which is the result of a combination of the applied stress and the accommodation strains induced by the characteristic shear and reorientation of the twin. These twin boundary strains are largely plastic [30–34] and alloying would influence the magnitude and extent of this stress field as well as the sensitivity of this field to crystallography of the parent and twin.

The relationships between alloying and the development of the twin microstructure at this scale have not been thoroughly explored. Systematic experimental studies would not be trivial, as alloying tends to change many other aspects of the microstructure that could affect the relative amounts of slip and twinning. Many mean-field polycrystal models, such as self-consistent schemes and the Taylor model, have been employed to treat constitutive behavior of many alloys [23,25,35–37]. Our recent work, for instance, employed the effective medium visco-plastic self-consistent (VPSC) model to study the effect of alloying additions on macroscopic plastic properties such as Lankford coefficients and tension-compression asymmetry ratio through the amounts of twinning activity [15]. However, while these polycrystal models allow for efficient calculations of bulk texture, stress-strain, and twin volume fractions, they do not capture details of the heterogeneous stress field of twin domains within a crystal or spanning a few crystals. Calculating the stress fields produced locally around a twin and inside its domain requires the use of spatially resolved crystal plasticity techniques. In this respect, full field crystal plasticity (CP) simulations, such as CP Finite Elements (CPFE) and Fast Fourier Transform (CP-FFT) [31,32,38–40], have an advantage over homogenization techniques since they can calculate the distribution of stress concentrations and their relationship to local microstructure.

In this work, the crystal plasticity Fast Fourier Transform-based (CP-FFT) model is employed to study the effect of alloying additions on the stress fields and in particular driving forces relevant for twin thickening and twin transmission. The effects of alloying are introduced here through the changes that alloying induces in the CRSS values of slip and twin systems. Based on these CRSS values, the same plastic anisotropy (PA) measure introduced in a previous mean-field polycrystal work [15] will be used to quantify the alloying effects. The analysis indicates that the high-PA alloys favor twin thickening and transmission, compared to alloys with the low-PA measure alloys. Also in low-PA alloys, these two modes of twin propagation are more sensitive to the orientation of the neighboring grains than high-PA alloys.

2. Modeling and analysis approach

2.1. Full field Fast Fourier Transform model

The particular CP-FFT approach used here is a recently advanced version to account for the twinning shear transformation associated with twin domains [31]. It has been used in prior to work to calculate the local stresses associated with finite size twin lamellae interacting with neighboring grains at grain boundaries for pure Mg [31,32]. The model calculates the stress state at each material point while accommodating the imposed deformation via crystal elasticity and plasticity. For reference, the constitutive model is briefly revisited below and for a general review of the mathematical formulation and solution procedures in CP-FFT we refer the reader to [40].

Material deformation follows elasto-viscoplastic constitutive behavior under an infinitesimal strain approximation with shear transformation, which can be written as

$$\boldsymbol{\sigma}(x) = \boldsymbol{C}(x)\colon \varepsilon^{\mathrm{el}}(x) = \boldsymbol{C}(x)\colon(\boldsymbol{\varepsilon}(x) - \boldsymbol{\varepsilon}^{\mathrm{pl}}(x) - \boldsymbol{\varepsilon}^{\mathrm{tr}}(x)) \tag{1}$$

where $\boldsymbol{\sigma}(x)$ is the Cauchy stress, $\boldsymbol{C}(x)$ is the elastic stiffness tensor, and $\boldsymbol{\varepsilon}^{\mathrm{el}}(x)$ is the elastic strain at material point x. The $\boldsymbol{\varepsilon}^{\mathrm{el}}(x)$ can be written as the difference between the total strain $\boldsymbol{\varepsilon}(x)$, and the plastic strain $\boldsymbol{\varepsilon}^{\mathrm{pl}}(x)$ due to crystallographic slip and the twinning transformation strain $\boldsymbol{\varepsilon}^{tr}(x)$.

We solve for the local stress field at material point $\boldsymbol{x}$ by using an implicit time discretization of the form:

$$\boldsymbol{\sigma}^{\mathrm{t}+\Delta\mathrm{t}}(x) = \boldsymbol{C}(x)\colon(\boldsymbol{\varepsilon}^{\mathrm{t}+\Delta\mathrm{t}}(x) - \boldsymbol{\varepsilon}^{\mathrm{pl,t}}(x) - \dot{\boldsymbol{\varepsilon}}^{\mathrm{pl,t}+\Delta\mathrm{t}}(x, \boldsymbol{\sigma}^{\mathrm{t}+\Delta\mathrm{t}})\Delta t - \boldsymbol{\varepsilon}^{\mathrm{tr,t}}(x) - \Delta\boldsymbol{\varepsilon}^{\mathrm{tr},\mathrm{t}+\Delta\mathrm{t}}(x)) \tag{2}$$

where,

$$\dot{\boldsymbol{\varepsilon}}^{\mathrm{pl}}(x) = \sum_{s=1}^{N} \boldsymbol{m}^{\mathrm{s}}(x)\dot{\gamma}^{\mathrm{s}}(x) \tag{3}$$

$$\dot{\gamma}^{\mathrm{s}}(x) = \dot{\gamma}_{\mathrm{o}}\left(\frac{|\boldsymbol{m}^{\mathrm{s}}(x)\colon\boldsymbol{\sigma}(x)|}{\tau_{\mathrm{o}}^{\mathrm{s}}}\right)^{\mathrm{n}} sgn(\boldsymbol{m}^{\mathrm{s}}(x)\colon\boldsymbol{\sigma}(x)) \tag{4}$$

where $\dot{\gamma}^{\mathrm{s}}$ and $\tau_{\mathrm{o}}^{\mathrm{s}}$ are, respectively, the shear rate and the critical resolved shear stress (CRSS) associated with slip systems s. In Eqs. (3)–(5), $\boldsymbol{m}^{\mathrm{s}} = \frac{1}{2}(\boldsymbol{b}^{\mathrm{s}}\otimes\boldsymbol{n}^{\mathrm{s}} + \boldsymbol{n}^{\mathrm{s}}\otimes\boldsymbol{b}^{\mathrm{s}})$, is the Schmid tensor and $\boldsymbol{b}^{\mathrm{s}}$ and $\boldsymbol{n}^{\mathrm{s}}$ are unit vectors along the Burgers vector and slip plane normal slip directions. The integer n is the stress exponent.

For points **x** within the twin domain, we build up the twin transformation strain by imposing the following change

$$\Delta\boldsymbol{\varepsilon}^{\mathrm{tr}}(x) = \boldsymbol{m}^{\mathrm{tw}}(x)\Delta\gamma^{\mathrm{tw}}(x) \tag{5}$$

where $\boldsymbol{m}^{tw} = \frac{1}{2}(\boldsymbol{b}^{tw}\otimes\boldsymbol{n}^{tw} + \boldsymbol{n}^{tw}\otimes\boldsymbol{b}^{tw})$ is the Schmid tensor associated with the twinning system. Unit vectors $\boldsymbol{b}^{tw}$ and $\boldsymbol{n}^{tw}$ are directed along the twinning direction and the twin plane normal, respectively. The twinning transformation is achieved via N^{twincr} increments of shear strain, according to

$$\Delta\gamma^{tw}(x) = \frac{s^{tw}}{N^{twincr}} \tag{6}$$

until the characteristic twinning shear s^{tw} is reached. The time increment, $\Delta t = 10^{-4}$s and the number of increments to achieve the twinning transformation N^{twincr} are set sufficiently low and high, respectively, to ensure convergence.

2.2. A measure for CRSS differences in Mg alloys

As mentioned above, alloying can cause a change in the CRSS values among the slip modes in the hcp crystal. Several measures have been presented for elastic anisotropy [41], but only a few for quantifying plastic anisotropy. One approach was presented by Yu et al. [42], who defined a ratio between non-basal to basal slip CRSS values as a plastic anisotropy (*PA*) measure. More specificity for non-basal modes would be needed, however, since more than one non-basal slip mode, e.g., prismatic $\langle a\rangle$ and pyramidal $\langle c+a\rangle$ slip, as well as tensile twinning, can contribute non-negligible amounts to accommodate plastic deformation. In prior work, we introduced a *PA* measure as the ratio of the difference in CRSS between the easier slip modes to the difference in CRSS between the easiest slip mode and tensile twinning [15]. For Mg, basal $\langle a\rangle$ slip is the easiest mode of slip and the next easiest is prismatic $\langle a\rangle$ slip and thus the *PA* measure would be given by:

$$PA = \frac{\tau_o^{\text{Prismatic}} - \tau_o^{\text{Basal}}}{\tau_o^{\text{TTwin}} - \tau_o^{\text{Basal}}} \tag{7}$$

where τ_0 is the CRSS value and the superscript indicates the slip or twin mode. This *PA* measure proved to be useful in correlating alloying effects on CRSS values with plastic anisotropy at the polycrystal level e.g., Lankford coefficients and tension-compression asymmetry ratio [15]. The intent of this *PA* measure was to facilitate analysis of Mg alloys, as opposed to offering a universal measure of plastic anisotropy for all alloys. As defined, it gauges slip relative to twinning. When $PA = 1$, prismatic $\langle a\rangle$ slip and tensile twinning have equal activation stresses and when $PA < 1$, slip is favored and vice versa when $PA > 1$. In this work, we employ this ad hoc measure to reflect how alloying additions adjust the relative activation stresses or CRSSs of prismatic slip and tensile twinning. That is, if a particular alloying addition inhibits the activity of tensile twinning, then it reduces plastic anisotropy, and vice versa.

2.3. Alloying elements in Mg and CRSS values for slip and twinning

To study the effect of alloying on twinning in Mg, five commonly studied Mg alloys shown in Table 1 were selected. In all five cases, alloying did not alter the HCP crystal structure of Mg and negligibly altered the elastic properties and lattice parameters.

Alloying, however, substantially altered their plastic properties. The corresponding CRSS values for the basal $\langle a\rangle$, prismatic $\langle a\rangle$ and pyramidal slip $\langle c+a\rangle$ slip modes, as well as tensile twinning are given in Table 2. Determining the slip-mode CRSSs for a given polycrystalline aggregate is not as straightforward as elastic moduli determination and are usually found via indirect methods. The CRSS values in Table 2 are obtained from applying crystal plasticity models using a hardening law based on the evolution of dislocation densities and fitting the hardening law parameters by matching predictions with the experimental measurements of deformation textures and stress-strain responses at the polycrystal level. These CRSS values were used to calculate a *PA* measure in Eq. (7) and are presented in Table 2. This measure varies widely among the selected five alloys, from 0.45 (small plastic anisotropy) to 23 (significant plastic anisotropy). Three are high- *PA* alloys with *PA* values above unity and three are low- *PA* alloys with *PA* values below unity.

Grain effects can be important when there are not sufficient numbers of grains (multi-crystals with large grains) or potentially different inelastic deformation mechanisms occur, such as in nanocrystalline materials. The grain sizes for the five alloys and pure Mg are also presented in Table 2. For the chosen five, tests were carried out on traditional polycrystalline grain structures with average grain sizes in the range of 10–100 μm.

Based on the above review, in the simulations that follow we set the c/a ratio and elastic modulus for Mg alloys in Table 1 to those for pure Mg at room temperature and ambient pressures, i.e., $c/a = 1.624$ and $C_{11} = 58.58$, $C_{12} = 25.02$; $C_{13} = 20.79$; $C_{33} = 61.11$; $C_{44} = 16.58$ (GPa) [45]. With a fixed c/a ratio, all five alloys and Mg will have the same characteristic twin shear s and twin plane for the $(10\bar{1}2)$ twin. Concerning elastic anisotropy, the values of the elastic modulus for an HCP Mg crystal give elastic anisotropy factors of 1.09, 1.01 and 1.23, where 1.0 represents isotropy [41][1], suggesting minimal elastic anisotropy. Consequently differences in the stress-strain fields and hence driving forces for twinning calculated by the CP-FFT model can be attributed to the effects of alloying on the plastic response.

2.4. Deformation simulations and reference twin resolved shear stress

2.4.1. Model set up

Fig. 2 shows a schematic of the 2D simulation cell, comprised of three grains surrounded by a layer with a uniformly random distributed texture. A twin lamella will be inserted into the parent grain (grain 1) that traverses from the boundary of one neighboring grain to the boundary of the other neighboring grain. The central parent grain orientation has its c-axis aligned with z-direction (see Fig. 2). Both neighbors have the same orientation (grain 2), which generally differs from the parent. To study the effect of neighboring grain on twinning, the central grain orientation will be fixed while the neighboring grains orientations are varied over the entire orientation space. Using increments of 10° produces 121 distinct neighboring grain orientations.

The simulation unit cell is discretized into $3\times510\times510$ voxels, and the buffer layer size is 20 voxels. This unit cell is sufficiently large to avoid the influence of boundary effects on the twinning in the central parent grain [31,32]. In actuality, twin lamellae form while the crystal is under stress. To mimic this situation, we first apply a stress state that would favor formation of a twin in the central crystal. In the present case, a compression stress along the y-axis, which, given the c-axis orientation of the central parent crystal, highly favors formation of the $(01\bar{1}2)[0\bar{1}11]$ twin variant. For Mg, the inclination of its twin boundary would be 43.1° with respect to the y-direction.

As the far-field compressive stresses on the twin-free tricrystal are applied and increased, the stress state in the outer polycrystalline layer and each of the three crystals develops. In all cases simulated, the stress states are uniform across each crystal but differ from grain 1 to grain 2 due to the differences in orientation and relative amounts of slip systems activated. After imposing initial compression along direction 2, a $\{10\bar{1}2\}$ tensile twin is introduced inside the central parent grain. To represent a newly formed fine lamella, the twin is made six voxels thick corresponding to a small twin volume fraction of 1.6%. Then the crystal orientations of those voxels are re-oriented to the twin-matrix relationship, and the characteristic twin shear of 13.0% is imposed over several increments [31].

[1] Anisotropic indices are defined as the ratios of the eigenvalues of the elastic stiffness tensor [41] as $\alpha = \frac{C_{11}+C_{12}-C_{22}}{C_{12}}$, $\beta = \frac{C_{66}}{C_{44}}$ and $\gamma = \frac{C^{(1)}}{2C_{44}}$. Where $C^{(1)} = \frac{C_{22}+C_{11}+C_{12}}{2} - \frac{C_{12}\sqrt{\alpha^2+8}}{2}$.

Table 1
Chemical composition of the studied magnesium alloys. RE stands for 'rare earth elements'.

Mg alloys	Chemical composition (wt%) of alloying elements and balance is Mg									Reference
	Al	Zn	Mn	Li	Zr	Ce	Y	Nd	Other REEs	
Pure Mg	–	–	–	–	–	–	–	–	–	[22]
AZ31	3.0	1.0	–	–	–	–	–	–	–	[43]
Mg4Li	–	–	–	4.0	–	–	–	–	–	[9]
ME21	–	–	2.0	–	–	0.7	–	–	–	[8]
ZK60A	–	4.8–6.2	–	–	0.5	–	–	–	–	[44]
WE54	–	–	–	–	–	–	5.0	1.6	2.6	[10]

Table 2
Critical resolved shear stress (CRSS) for basal, prismatic, pyramidal and tensile twin deformation modes of the studied magnesium alloys along with grain size. The CRSS values are obtained from the crystal plasticity modeling literature.

Mg alloys	Grain size (micron)	Method / Tool	Initial CRSS values [MPa]				PA measure	Reference
			Basal	Prismatic	Pyramidal	T. Twin		
Mg4Li	5 & 30	EPSC	5	14	52	25	0.45	[9]
WE54	17–20	EPSC	10	80	115	115	0.67	[10]
ME21	10–30	EPSC	10	37	50	39	0.93	[8]
Pure Mg	20–100	VPSC	3.33	35.7	86.2	20.0	1.94	[22]
ZK60A	10–30	EVPSC	40	115	125	56	4.69	[44]
AZ31	13	CPFE	11.6	46.82	157.02	12.8	29.35	[43]

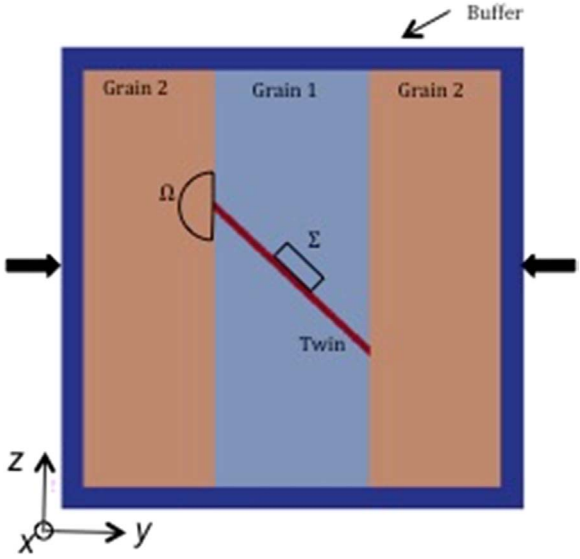

Fig. 2. Schematic representation of the tri-crystal simulation unit cell. The twin is embedded in a central grain (grain 1) and the twin front is arrested at the grain boundary with the neighboring grain (grain 2). A buffer layer with random crystal orientations surrounds the tri-crystal. This configuration represents a polycrystal in which only three grains are magnified for numerical simulation purposes. The region Ω in the neighboring grain is the potential region where twin transmission may occur and where the stresses available for twin transmission are calculated. The region Σ in the middle of the twin boundary is the potential region where twin growth may occur.

Inserting a twin at a given stress implies that the stress state in the parent crystal is sufficiently high to support formation and propagation of the $(01\bar{1}2)[0\bar{1}11]$ twin across the grain. The critical stress to form the twin is challenging to determine, and it might not be a singular value covering all stages in the twin embryo to lamella process, or deterministic, i.e. constant from twin to twin. The character of this stress is unknown as well, and would correspond to the driving forces needed to expand the twin and migrate the twin boundary. These driving forces depend on the specific defect configuration at the twin-parent interface, their activation barriers, and their mobility [46]. In this work, we use for a driving force to move the twinning dislocations along the twin boundary the stress projected onto the twin plane and in the twinning direction, i.e., the twin resolved shear stress (TRSS).

The actual value of the TRSS at which twins form is naturally statistically varying. Different assumptions can be made to define a reasonable critical TRSS for twin growth. In this work, the twin is inserted when the TRSS in the parent crystal rises above the CRSS for $\{10\bar{1}2\}$ twinning (Table 2). Thus the TRSS at which the twin is inserted is arbitrarily above the CRSS and defined here as a *reference stress,* τ_{ref}. After twinning, we can increase the applied load and calculate the local rise in the stresses along the twin boundary. As a criterion for twin growth we assume that the local TRSS at the twin boundary must reach or exceed τ_{ref}. We use this criterion consistently in all simulations as the orientations of the neighboring crystals change.

3. Results

3.1. Effect of PA on the self-suppressing twin backstress

In order to represent a full picture, the entire space of neighbor orientations is tested. Calculations of the micromechanical fields (stress, strain, strain rate) generated around twins are performed for all Mg alloys. For each alloy, the calculations are repeated with 121 distinct neighboring grains. Fig. 3(a) shows a typical TRSS distribution, using the AZ31 Mg alloy with (0°, 70°, 0°) neighboring grain orientation as an example. The field is heterogeneous, possessing a negative TRSS in the vicinity of the twin in the parent and positive TRSS (in the twin direction) in the neighboring grains, particularly near the twin tips.

To better determine how this field could impact further twin expansion, we plot the corresponding TRSS profile along twin boundary in Fig. 3(b). The lowest and highest values of TRSS occur where the twin tip meets the grain boundary, with the former in the parent and the latter in the neighbor. The TRSS increases from the tip along the twin boundary to the center of the parent grain, where it plateaus. The difference in the TRSS in this region, before and after twinning, is denoted here as a backstress.

To demonstrate the effect of alloying we show the same calculation for the same parent-neighbor orientation relationship for pure Mg and WE54 Mg alloy in Fig. 3(c) and (d), respectively. We selected these since pure Mg has a lower *PA* measure than WE54 and even lower value compared to AZ31. Despite the stark contrast in *PA* measure, the stress

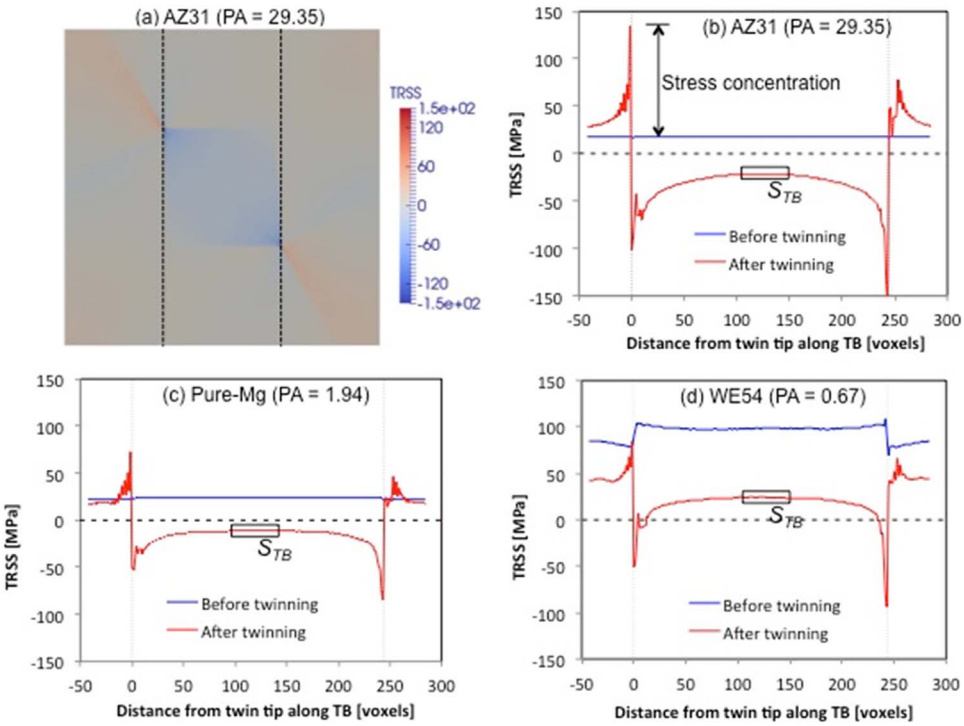

Fig. 3. (a) Twin plane resolved shear stress (TRSS) distribution after twinning in AZ31 Mg alloy. The TRSS profile along twin boundary before and after twinning for (b) AZ31 Mg alloy, (c) pure Mg, and (d) WE54 Mg alloy. The neighboring grain orientation for all three cases is same as (0°, 70°, 0°).

field bears the same form. Taking the TRSS as a potential driving force, the neighboring grain experiences a stress that could favor further twin expansion, even if it were not oriented well for this twin variant. On the other hand, the parent grain, originally well oriented for this twin variant, experiences a TRSS that opposes further twin growth. This trend is characteristic of the twin/parent/neighbor configuration and likely applies to all cases of Mg and its alloys.

3.2. Twin thickening

As seen in the prior section, under the current applied τ_{ref}, the local stress state near the twin is not conducive for growth; the sense of TRSS at the twin tips and along the twin boundary in the parent grain acts against twinning. The anti-twinning (negative) value is highest at the tips and reduces towards the center. To thicken the twin, the applied

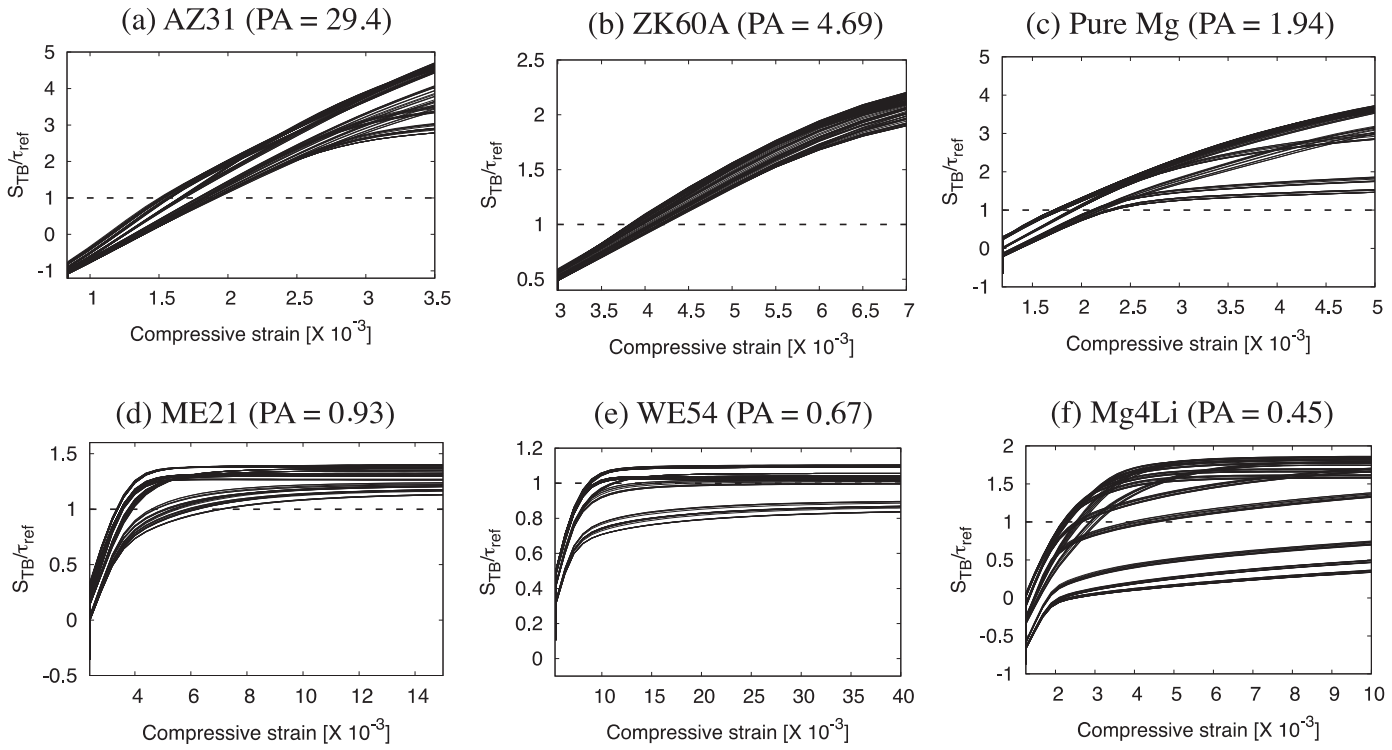

Fig. 4. Evolution of the ratio between the average TRSS in the region Σ (see Figs. 2 and 3) in twin boundary middle, S_{TB}, and reference stress (τ_{ref}) of (a) AZ31, (b) ZK60A, (c) pure Mg, (d) ME21, (e) WE54 and (f) Mg4Li. Different curves in each plot correspond to different neighboring grain. The normalization reference stress (τ_{ref}) for tensile twin systems is same as the CRSS values for tensile twins presented in Table 2.

load would need to be increased to a level that causes the local stress state acting at the twin boundary, to reach or exceed τ_{ref}. To estimate the corresponding additional applied load needed to reach or exceed τ_{ref}, we track the evolution of S_{TB} (see Fig. 3(d)) as we further increase the load. S_{TB} is the TRSS averaged within a region Σ in the middle of the twin, where the local stress is the highest (see Fig. 1). The initial difference between S_{TB} and τ_{ref} is referred to as a backstress.

Fig. 4 shows the increase in S_{TB} (normalized with the reference stress, τ_{ref} at which the twin was first introduced) as the compressive strain in the y-direction increases. Each plot refers to a single alloy and the individual curves for a given alloy corresponds to a different neighboring grain orientation. When S_{TB}/τ_{ref} reaches unity, the TRSS at the boundary has recovered to its original value at the moment the twin was introduced. According to the criterion discussed earlier, values of S_{TB}/τ_{ref} above unity are viewed here as a favorable state to expand the twin in region Σ. In all cases, for the load when the twinning occurs, S_{TB}/τ_{ref} is less than one and increases as the applied strain increases.

Whether S_{TB}/CRSS = 1 is achieved depends on alloying and local neighborhood. For alloys with $PA > 1$, which are here AZ31, ZK60A, and pure Mg, it is possible to increase the applied strain until - a critical value is reached such that S_{TB}/S_R exceeds unity. The value of critical strain for these alloys displays some dependence on neighborhood, but generally the spread is small. In contrast, for alloys with lower *PA*, such as ME21, WE54 and Mg4Li, the evolution of S_{TB}/τ_{ref} is sensitive to neighborhood. For some orientations, the critical strain is relatively large, even to the point where S_{TB}/τ_{ref} does not reach unity under further straining. The saturation in S_{TB}/τ_{ref} is a likely consequence of the lack of hardening of the CRSS in the model. Nonetheless, the sensitivity of twin growth to neighboring orientation clearly decreases as *PA* increases.

To see this trend, Fig. 5 presents the critical strain to reach $S_{TB}/\tau_{ref} = 1$ for all neighboring orientations, plotted as a function of *PA*. For the high *PA* -measure alloys, namely AZ31, ZK60A and pure Mg, the critical strain required is less than 0.15%, and the variation among neighboring grain orientations is also small. For ME21, with a value of *PA* slightly below one, the required additional strain for twin thickening ranges from 0.12% to 0.48% and a strong dependence of neighboring grain orientation emerges. For WE54 and Mg4Li, not all the neighboring grain orientations allow for the possibility of twin thickening. Only 76% and 72% of the cases for WE54 and Mg4Li, respectively, provide for the possibility of twin thickening. In essence, high *PA* -measure alloys are more prone to expand the twin under an increasing applied strain (or stress) and this tendency exhibits less sensitivity to neighboring grain orientation compared to low *PA* -measure alloys.

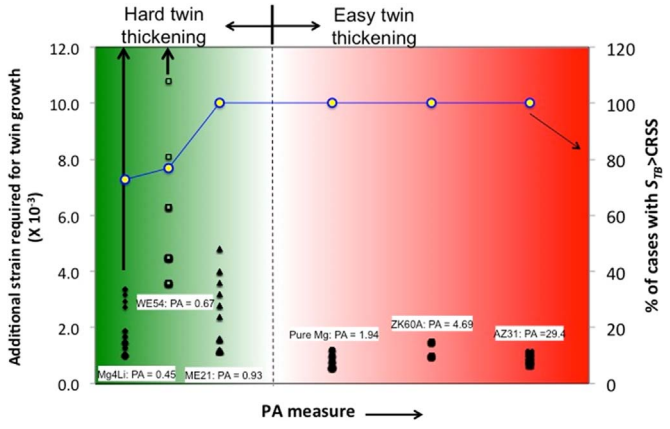

Fig. 5. Effect of alloying represented in terms of plastic anisotropic (PA) measure, on twin growth in magnesium alloys. The first vertical axis shows the amount of additional strain required to start the twin growth process for different neighboring grains, i.e., the strain at which S_{TB} > CRSS. The second vertical axis shows the percentage of cases where twin growth is observed.

3.3. Twin transmission

As we have seen in the calculations presented in Section 3.1, the tips of twins stopped at a grain boundary can produce stress concentrations in the neighboring crystals. This stress concentration from one twin can act as a driving force for forming a new twin in the neighboring grain at the twin/grain boundary intersection. Signatures of this event can appear as adjoining twin pairs (ATPs) or as a chain of connected twins. Compared to single twins, ATPs have a heightened ability to resist detwinning, act as a potential site for crack and void formation, or provide a path for inter-grain crack propagation or shear banding [27–29]. Characterization studies involving large data sets of ATPs in pure metals have shown that they tend to occur at boundaries with low grain boundary misorientation. Previously the CP-FFT model was applied to these pure metals (HCP Mg, Zr and Ti) to study whether stress fields produced at twin tips can explain how and why ATPs happen [47].

The stress concentrations generated at the tip are extended over a finite region. For practical quantification of a driving force for a new twin, we average the TRSS in a small region at the twin tip (marked as region Ω in Fig. 2), with a radius equal to the thickness of the twin. The maximum averaged TRSS in Ω among all six tensile twin variants, denoted as the $TRSS_{tip}$, is retained as a measure of the driving force for twin propagation. The calculation for $TRSS_{tip}$ is repeated for each of the 121 neighboring orientations.

A distinctive situation among these cases considers an internal twin of the same morphology embedded completely inside the parent grain. Both twin tips lie within the single crystal and have yet to reach the ends of the crystal or grain boundaries. As the crystal studied here is optimally oriented for twinning, it is expected that the $TRSS_{tip}$, specially denoted as $TRSS_{SX}$, would be sufficient to propagate the twin to the ends of the crystal without any further increase in load. For this reason, $TRSS_{SX}$ is used as an ideal reference state for propagating a twin with whom all other $TRSS_{tip}$ are compared. As the central parent grain is ideally oriented for twinning, any deviating neighboring orientations would not be as well oriented under the same loading state and so $TRSS_{ratio} = TRSS_{tip}/TRSS_{SX}$ is expected to be less than one. A value of unity implies that the driving force for twinning in the neighboring grain at the tip of the twin is equal to that for twin propagation of the same twin in its parent crystal.

Fig. 6 shows the variation in $TRSS_{ratio}$ with the misorientation angle between the parent and the neighboring grain. This map is compared for all six alloys. There are many similarities. For all six the $TRSS_{ratio}$ decreases with misorientation angle, suggesting that the tendency for ATP formation decreases with increasing misorientation angle. This general trend is seen experimentally in pure metals as well as in similar calculations [47,48]. However, the CRSS differences, as affected by alloying, are seen to change many other details of these maps, suggesting an alloying effect on ATP propensity. First, for every alloy, the $TRSS_{ratio}$ for some neighboring orientations remains near 1.0 for a low misorientation interval 0 to $\Delta\theta_c$, and decreases below 1.0 with increasing grain boundary misorientation angle. Larger $\Delta\theta_c$ values are associated with larger *PA* alloys. The values of $\Delta\theta_c$ for AZ31, ZK60A, and pure Mg are 30°, 15°, and 20°, respectively. Likewise, smaller *PA* alloys ($PA < 1$) have shorter ranges, or smaller $\Delta\theta_c$. For AZ31 we note that in this range, $TRSS_{ratio}$ can exceed one, suggesting that the driving force to propagate a twin in the neighbor is greater than that to propagate a twin in its own crystal. Previously this effect was linked to large differences in CRSS between the slip modes and not to the elastic anisotropy of the crystal [47]. This result supports our previous work conclusion in that all alloys here had the same elastic response and only the alloy with the greatest differences in CRSS exhibited this "transmission boost" effect. Secondly, the misorientation angle is not a complete description of the grain boundary character. Therefore the same misorientation angle $\Delta\theta$ can be achieved with different neighboring orientations. The lower *PA* alloys, WE43 and Mg4L, exhibit a

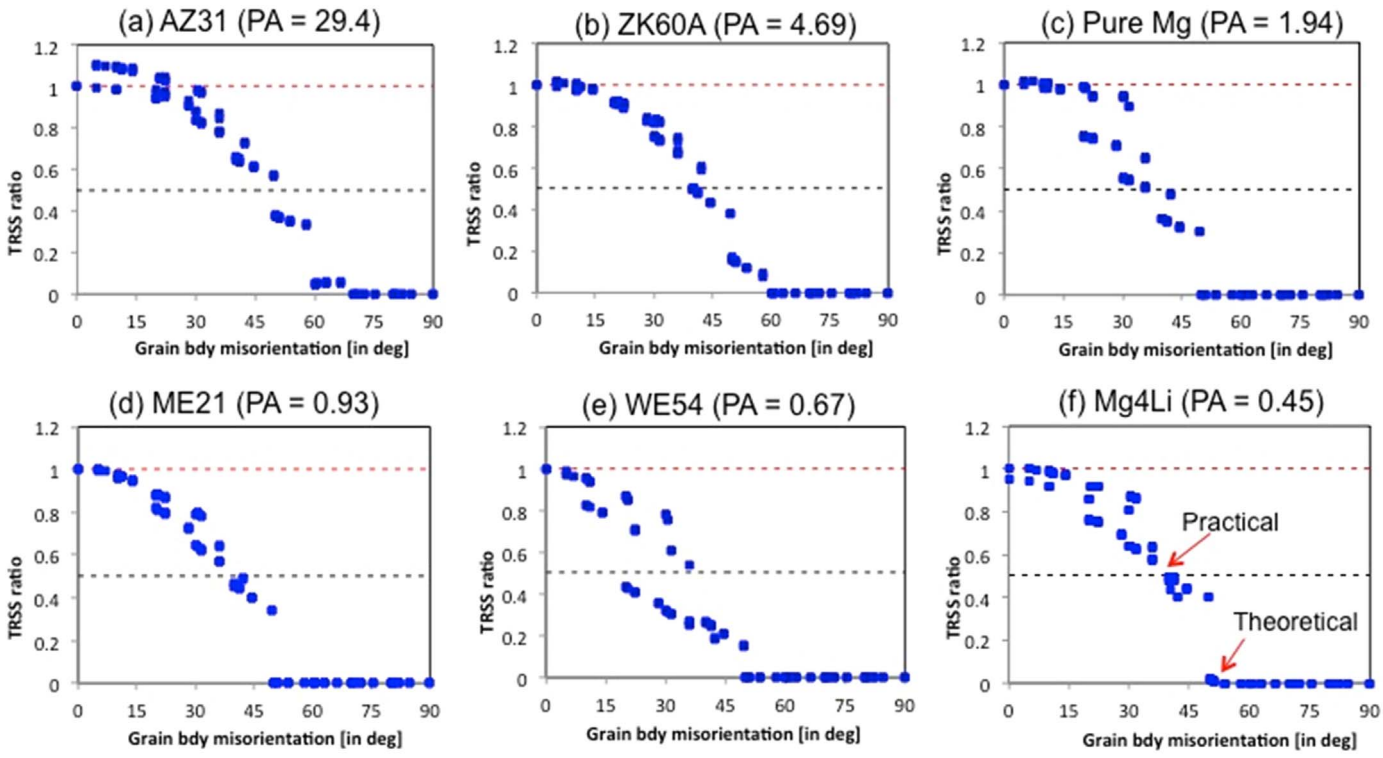

Fig. 6. Evolution of the $TRSS_{ratio}$ ($=TRSS_{\Omega}/TRSS_{SX}$) in the region Ω (see Fig. 2) as a function of misorientation at grain boundary for (a) AZ31, (b) ZK60A, (c) pure Mg, (d) ME21, (e) WE54 and (f) Mg4Li.

greater sensitivity to neighboring orientations than others, indicated by a spread in the $TRSS_{ratio}$ for the same $\Delta\theta$, particularly in the low $\Delta\theta$ regime where ATP formation is generally more likely. Last, a high (or too high) misorientation regime is well marked by a cut-off misorientation angle $\Delta\theta_{cut}$, above which the $TRSS_{ratio}$ is zero and chances for ATP formation nil. In these maps $TRSS_{ratio} = 0$ corresponds to a calculated maximum averaged TRSS at the tip of zero or negative. Taken together, these indicators point to high *PA* alloys, bearing microscopically larger differences in CRSS among the easier slip modes, as being more prone to develop the driving forces to form ATPs.

To more directly appreciate effect of alloying addition on twin transmission, the value of $\Delta\theta_{cut}$ with *PA* is mapped in Fig. 7. For higher *PA* alloys, $\Delta\theta_{cut}$ increases with *PA*, while for lower *PA* alloys, $\Delta\theta_{cut}$ is fixed at a low value of ~ 50°. This value is close to the 55° value based on geometry only, the cut off angle above which either the twin directions or planes of the twin pair on either side of the grain boundary are not aligned [47]. We can arbitrarily define another cut-off angle, associated with $TRSS_{ratio} = 0.5$, which is arguably a more practical choice than $\Delta\theta_{cut}$ since this angle corresponds to a neighboring grain that bears a driving force that is 50% lower than that to propagate a twin in its own parent crystal. These more practical cut-off angle definition follows the same variation with *PA* as seen in Fig. 7. However, this 50%-chance misorientation angle is more likely to be consistent with experimental observations. It is reasonable to expect that crossed twins would rarely be seen, particularly when the data sets are small, for misorientation corresponding to $TRSS_{ratio} = 0.5$, which are 36° for the low *PA* alloys and ~ 50° for the highest one.

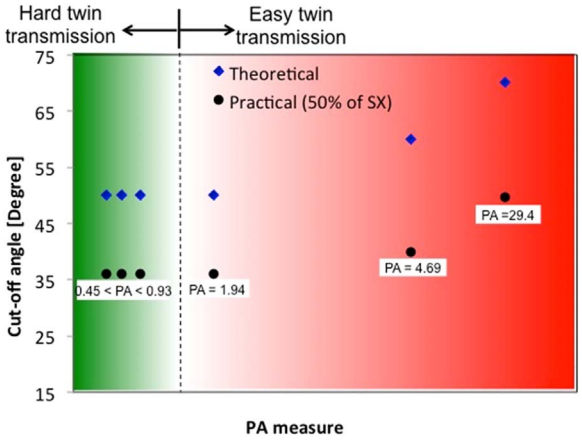

Fig. 7. Effect of alloying addition on twin transmission, represented by cut-off angles, in magnesium alloys. Theoretical and practical cut-off angle corresponds to the grain boundary misorientation angle at which the TRSS ratio is 0.0 and 0.5, respectively (see Fig. 6(f)).

4. Discussion

Polycrystal modeling has shown that one of the main influences of alloying is to change the CRSS values among the various slip modes used by HCP crystals [9,10,43,49]. The full-field elastic-viscoplastic crystal plasticity calculations in this work strongly suggest that differences in CRSS values among the easier slip modes compared to differences between slip and twinning CRSS can greatly affect the propagation of a twin lamella. Presuming that all alloys can at least produce a fine-scale twin that spans the grain, these calculations show that further thickening of the twin and triggering another twin in a neighboring crystal, depends sensitively on slip. Plastic slip accommodates the characteristic twin shear imposed by the twin lamella. Larger differences in CRSS provide higher driving forces for both self-thickening and inducing new twinning in neighboring grains. Additions of Li and rare earth elements like Y, Nd, have been shown to reduce these differences [9,10,49] whereas addition of Al tends to increases them, giving tensile twin more opportunity to be formed [9]. In terms of the *PA* measure introduced here, Al-added AZ31 Mg alloy correlates with a high- *PA* alloy, while Li-added Mg4Li alloy and Y-added WE54 alloys correlate to low- *PA* alloys. Provided a fine twin already is present in these alloys,

plastic accommodation of this twin lamella could drive twin thickening and transmission in the high- *PA* alloy and less so in the low- *PA* alloys.

Generally, smaller difference in CRSSs values among the slip modes are known to be desirable for their association with greater formability and weaker deformation texture development. Here we find that, apart from formability, other important consequences of alloying effects on CRSS can arise. In particular, the original implication of these studies is that alloying can have a more direct effect on twin morphologies than first thought. Hindrance of twin thickening and promotion of finer twins can help in designing alloys that form twin networks within grains. Hindrance of twin transmission via alloying can help to prevent twin chains from forming and acting as preferred paths for subsequent shear banding or cracking.

5. Conclusions

Crystal plasticity based full-field Fast Fourier Transform (FFT) model is applied to study the effect alloying additions in magnesium alloys on twin thickening and twin transmission. The alloying effect is accounted through microscopic level CRSS values of slip and twinning deformation modes. To quantify the alloying effect, a plastic anisotropy (*PA*) measure is formulated using the CRSS values of slip and twin systems. The alloys with high *PA* measure favor twin thickening and twin transmission, while the opposite applies for those with low *PA* measure. Also the neighboring grain dependence is strong for low *PA* measure alloys and almost negligible for high *PA* measure alloys. These results provide an unprecedented aspect of alloying that can benefit alloy design, particularly with twinning, strength, formability and ductility in mind.

Acknowledgments

This work is fully funded by the U.S. Dept. of Energy, Office of Basic Energy Sciences Project FWP 06SCPE401. IJB acknowledges financial support from the National Science Foundation Designing Materials (CMMI-1729887) to Revolutionize and Engineer our Future (DMREF) program (NSF CMMI-1729887).

References

[1] A. Akhtar, Plastic deformation of Zr single crystals, Acta Metall. 19 (1971) 655.
[2] P.G. Partridge, The crystallography and deformation modes of hexagonal close-packed metals, Metall. Rev. 12 (1967) 169–194.
[3] M.H. Yoo, Slip, twinning and fracture in Hexagonal Close Packed metals, Met. Trans. 124 (1981) 409.
[4] M.H. Yoo, J.H. Lee, Deformation twinning in hexagonal close-packed metals and alloys, Philos. Mag. 63A (1991) 987–1000.
[5] M.H. Yoo, S.R. Agnew, J.R. Morris, K.M. Ho, Non-basal slip systems in HCP metals and alloys: source mechanisms, 319-321319–321, Mater. Sci. Eng. A (2001) 87–92.
[6] A. Ghaderi, F. Siska, M.R. Barnett, Influence of temperature and plastic relaxation on tensile twinning in a magnesium alloy, Scr. Mater. 69 (2013) 521–524.
[7] I.J. Beyerlein, C.N. Tomé, A dislocation based constitutive law for pure Zr including temperature effects, Int J. Plast. 24 (2008) 867–895.
[8] M. Lentz, M. Klaus, R.S. Coelho, N. Schaefer, F. Schmack, W. Reimers, B. Clasuen, Analysis of the deformation behavior of magnesium-rare earth alloys Mg-2 pct Mn-1 pct rare earth and Mg-5 pct Y-4 pct rare earth by in situ energy-dispersive x-ray synchrotron diffraction and elasto-plastic self-consistent modeling, Metall. Mater. Trans 45A (2014) 5721–5735.
[9] M. Lentz, M. Klaus, I.J. Beyerlein, M. Zecevic, W. Reimers, M. Knezevic, In situ X-ray diffraction and crystal plasticity modeling of the deformation behavior of extruded Mg-Li-(Al) alloys: an uncommon tension-compression asymmetry, Acta Mater. 86 (2015) 254–268.
[10] M. Lentz, M. Klaus, M. Wagner, C. Fahrenson, I.J. Beyerlein, M. Zecevic, W. Reimers, M. Knezevic, Effect of age hardening on the deformation behavior of an Mg-Y-Nd alloy: in situ X-ray diffraction and crystal plasticity, Mater. Sci. Eng. A628 (2015) 396–409.
[11] R.J. McCabe, E.K. Cerreta, A. Misra, G.C. Kaschner, C.N. Tomé, Effects of texture, temperature and strain on the deformation modes of zirconium, Philos. Mag. A86 (2006) 3595–3611.
[12] S. Ando, M. Tsushida, H. Kitahara, Plastic deformation behavior in magnesium alloy single crystals, Mater. Sci. Forum 706–707 (2012) 1122–1127.
[13] A. Chakkedath, J. Bohlen, S. Yi, S. Letzig, Z. Chen, C.J. Boehlert, The effect of Nd on the tension and compression deformation behavior of extruded Mg-1Mn (wt pct) at temperatures between 298 K and 523 K (25 C and 250 C), Metall. Mater. Trans 45A (2014) 3254–3274.
[14] S.R. Agnew, M.H. Yoo, C.N. Tomé, Application of texture simulation to understanding mechanical behavior of Mg and solid solution alloys containing Li or Y, Acta Mater. 49 (2001) 4277–4289.
[15] M. Arul Kumar, I.J. Beyerlein, C.N. Tomé, A measure of plastic anisotropy for hexagonal close packed metals: application to alloying effects on the formability of Mg, J. Alloy. Compd. 695 (2017) 1488–1497.
[16] M. Arul Kumar, I.J. Beyerlein, R.A. Lebensohn, C.N. Tomé, Modeling the effect of alloying elements in magnesium on deformation twin characteristics, in: K. Solanki, D. Orlov, A. Singh, N. Neelameggham (Eds.), Magnesium Technology 2017, The Minerals, Metals and Materials Series, Springer, 2017, pp. 159–165.
[17] L. Capolungo, I.J. Beyerlein, C.N. Tomé, Slip-assisted twin growth in hexagonal close packed metals, Scr. Mater. 60 (2009) 32–35.
[18] A. Serra, D.J. Bacon, A new model for {10-12} twin growth in hcp metals, Philos. Mag. A73 (1996) 333–343.
[19] J. Wang, I.J. Beyerlein, C.N. Tomé, An atomic and probabilistic perspective on twin nucleation in Mg, Scr. Mater. 63 (2010) 741–746.
[20] J.J. Bhattacharya, F. Wang, P.D. Wu, W.R. Whittington, H. El Kadiri, S.R. Agnew, Demonstration of alloying, thermal activation, and latent hardening effects on quasi-static and dynamic polycrystal plasticity of Mg alloy, WE43-T5 plate, Int. J. Plast. 81 (2016) 123–151.
[21] Y.B. Chun, C.H.J. Davies, Twinning induced negative strain rate sensitivity in wrought Mg all AZ31, Mater. Sci. Eng. A 528 (2011) 5713–5722.
[22] I.J. Beyerlein, R.J. McCabe, C.N. Tomé, Effect of microstructure on the nucleation of deformation twins in polycrystalline high-purity magnesium: a multiscale modeling study, J. Mech. Phys. Solids 59 (2011) 988–1003.
[23] B. Clausen, C.N. Tomé, D.W. Brown, S.R. Agnew, Reorientation and stress relaxation due to twinning: modeling and experimental characterization for Mg, Acta Mater. 56 (2008) 2456–2468.
[24] G. Proust, C.N. Tomé, G.C. Kaschner, Modeling texture, twinning and hardening evolution during deformation of hexagonal materials, Acta Mater. 55 (2007) 2137–2148.
[25] H. Wang, P.D. Wu, J. Wang, C.N. Tomé, A crystal plasticity model for HCP crystals including twinning and detwinning mechanisms, Int. J. Plast. 49 (2013) 36–52.
[26] H. Fan, S. Aubry, A. Arsenlis, J.A. El-Awady, The role of deformation twinning on the hardening response of polycrystalline magnesium from discrete dislocation dynamics simulations, Acta Mater. 92 (2015) 126–139.
[27] B.A. Simkin, M.A. Crimp, T.R. Bieler, Crack opening due to deformation twin sheet at grain boundaries in near gamma-TiAl, Intermetallics 15 (2007) 55–60.
[28] F. Yang, S.M. Yin, S.X. Li, Z.F. Zhang, Crack initiation mechanism of extruded AZ31 magnesium alloy in the very high cycle fatigue regime, Mater. Sci. Eng. A 491 (2008) 131–136.
[29] S.M. Yin, F. Yang, X.M. Yang, S.D. Wu, S.X. Li, G.Y. Li, The role of twinning and detwinning on fatigue fracture morphology of Mg-3%Al-1%Zn alloy, Mater. Sci. Eng. A 494 (2008) 397–400.
[30] M. Ardeljan, R.J. McCabe, I.J. Beyerlein, M. Knezevic, Explict incorporation of deformation twins into crystal plasticity finite element models, Comput. Methods Appl. Mech. Eng 295 (2015) 396–413.
[31] M. Arul Kumar, A.K. Kanjarla, S.R. Niezgoda, R.A. Lebensohn, C.N. Tomé, Numerical study of the stress state of a deformation twin in magnesium, Acta Mater. 84 (2015) 349–358.
[32] M. Arul Kumar, I.J. Beyerlein, C.N. Tomé, Effect of local stress fields on twin characteristics in HCP metals, Acta Mater. 116 (2016) 143–154.
[33] M. Arul Kumar, I.J. Beyerlein, R.A. Lebensohn, C.N. Tomé, Neighboring grain dependence on twin on twin local stresses and twin thickening in HCP metals, Model. Simul. Mater. Sci. Eng. 25 (2017) 064007.
[34] M. Knezevic, M.R. Daymond, I.J. Beyerlein, Modeling discrete twin lamellae in a micro structural framework, Scr. Mater. 121 (2016) 84–88.
[35] R.A. Lebensohn, C.N. Tomé, Modelling twinning in texture development codes, Textures Microstruct. 14 18 (1991) 959–964.
[36] R.A. Lebensohn, C.N. Tomé, A self-consistent anisotropic approach for the simulation of plastic deformation and texture development of polycrystals – application to zirconium alloys, Acta Metall. Mater. 41 (1993) 2611–2624.
[37] S.R. Niezgoda, A.K. Kanjarla, I.J. Beyerlein, C.N. Tomé, Stochastic model of twin nucleation in polycrystals: an application to hexagonal close packed metals, Int. J. Plast. 56 (2014) 119–138.
[38] H. Abdolvand, M.R. Daymond, Multi-scale modeling and experimental study of twin inception and propagation in HCP materials using a crystal plasticity finite-element approach – Part I: average behavior, J. Mech. Phys. Solids 61 (2013) 783–802.
[39] H. Abdolvand, M. Majkut, J. Oddershede, J.P. Wright, M.R. Daymond, Study of 3-D stress development in parent and twin pairs of a hexagonal close packed polycrystal: Part II crystal plasticity finite element modeling, Acta Mater. 93 (2015) 235–245.
[40] R.A. Lebensohn, A.K. Kanjarla, P. Eisenlohr, An elasto-visco-plastic formulation based on Fast Fourier transforms for the prediction of micromechanical fields in polycrystalline materials, Int J. Plast. 32–33 (2012) 59–69.
[41] U.F. Kocks, C.N. Tomé, H.R. Wenk, Texture and Anisotropy – Preferred Orientations in Polycrystals and their Effect on Materials Properties, 2nd edition, Cambridge University Press, 2000.
[42] Q. Yu, L. Qi, R.K. Mishra, J. Li, A.M. Minor, Reducing deformation anisotropy to achieve ultrahigh strength and ductility in Mg at the nanoscale, Proc. Natl. Acad. Sci. USA 110 (2013) 13289–13293.
[43] M. Ardeljan, I.J. Beyerlein, B.A. McWilliams, M. Knezevic, Strain rate and temperature sensitive multi-level crystal plasticity model for large plastic deformation behavior: application to AZ31 magnesium alloy, Int J. Plast. 83 (2016) 90–109.

[44] H. Qiao, S.R. Agnew, P.D. Wu, Modeling twinning and detwinning behavior of Mg alloy ZK60A during monotonic and cyclic loading, Int. J. Plast. 65 (2015) 61–84.
[45] G. Simmons, H. Wang, Single Crystal Elastic Constants and Calculated Aggregate Properties: A Handbook, The MIT press, 1971.
[46] J.P. Hirth, J. Wang, C.N. Tome, Disconnections and other defects associated with twin interfaces, Prog. Mater. Sci. 83 (2016) 417–471.
[47] M. Arul Kumar, I.J. Beyerlein, R.J. McCabe, C.N. Tomé, Grain neighbor effects on twin transmission in hexagonal close packed materials, Nat. Commun. 7 (2016) 13826.
[48] I.J. Beyerlein, L. Capolungo, P.E. Marshall, R.J. McCabe, C.N. Tomé, Statistical analyses of deformation twinning in magnesium, Philos. Mag. 90 (2010) 2161–2190.
[49] J. Bohlen, S. Yi, D. Letzig, K.U. Kainer, Effect of rare earth elements on the microstructure and texture development in magnesium–manganese alloys during extrusion, Mater. Sci. Eng. A527 (2010) 7092–7098.